Proceedings of the International Conference on
Interstitial-free Steels

Jamshedpur, India, 2010

Phase Transformations during Spot Welding of Interstitial–Free Steel

H. K. D. H. Bhadeshia

University of Cambridge
Materials Science and Metallurgy
Pembroke Street, Cambridge CB2 3QZ, U. K.

Abstract

It is often difficult to understand the microstructures that develop in low–carbon steels because of the rapidity with which austenite transforms into ferrite. The microstructural features that develop during the resistance spot–welding of interstitial–free steels are exceptionally problematic, not only because of the speed of transformation but also the short time–scales of the welding process itself. A methodology, based on phase transformation theory, is presented here to enable the interpretation of the gradients of microstructure in the weld nugget and its associated heat–affected zone.

1 Introduction

Structure–property relationships relationships are most useful when it becomes possible to control the development of microstructure. This in turn requires a knowledge of the mechanisms of phase transformation, since without this information, one is reduced to simply naming the microstructures that are observed. Many naming schemes exist for low–carbon steels, for example, [1, 2], but they tend to neglect atomistic phenomena and hence are only useful in communicating structure rather than predicting it. The purpose of this paper is to provide a methodology based on the principles of phase transformation theory to help identify the phases that form when interstitial free steels are resistance spot–welded.

Interstitial–free steels do in reality contain traces of carbon and nitrogen, but the concentrations are very small and are gettered by the use of strong carbonitride forming elements such as titanium and niobium, Table 1. They are not particularly strong but can be formed by pressing, and hence are useful in the automotive industry.[1] When they are used for outer body panels, the painting

[1]Their formability is usually discussed in terms of the Lankford ratio, which is given approximately by the plastic strain measured in the plane of a sheet tensile–specimen divided by the plastic strain in the thickness direction; a large ratio corresponds to greater formability since thinning is minimised during pressing. The ratio varies with the angle of the tensile axis relative to the rolling direction. In interstitial–free steels the ratio is in the range 1.6–2.1.

stage introduces bake hardening, thus making these panels more resistant to denting.

The assembly of the so–called body–in–white requires joining technologies, the most popular of which is resistance spot welding, although laser welding and indeed adhesive bonding are making inroads.

2 Phase Diagram

Calculated equilibrium phase fractions as a function of temperature [6] for an interstitial–free steel containing titanium, are illustrated in Fig. 1a. The first thing to notice is that the temperature range (≃870–890°C) over which austenite and ferrite coexist is minimal because of the very low solute concentrations in the alloy. The quantity of titanium carbide remains almost constant in the ferrite phase field but its solubility in austenite is much greater, so that it does not exist as an equilibrium phase for temperatures in excess of 950°C. The purpose of elements such as titanium and niobium is to combine with the carbon and render the ferrite virtually free from dissolved carbon. Note that the austenite transforms completely into δ–ferrite at temperatures in excess of 1400°C.

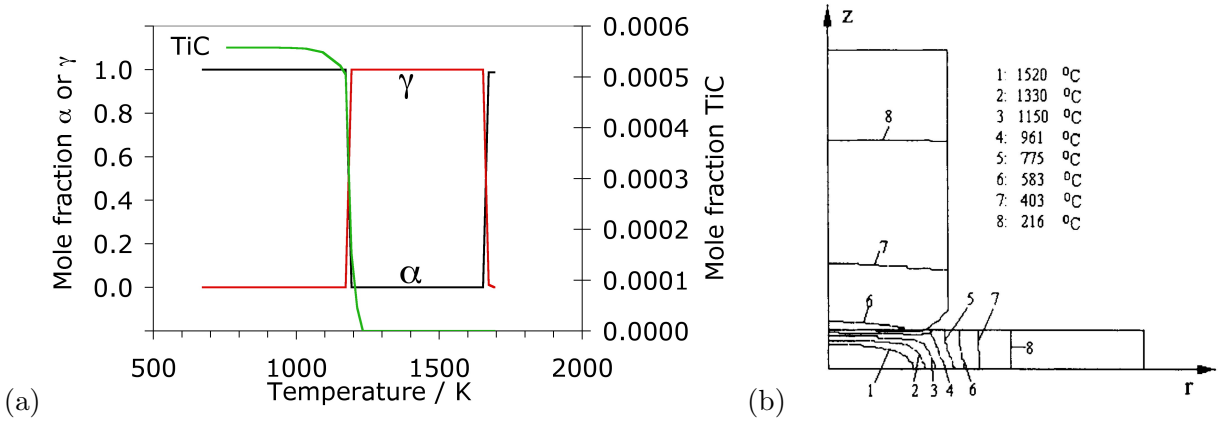

Figure 1: (a) Calculated phase diagram for an interstitial–free steel of chemical composition Fe-0.006C-0.183Mn-0.057Al-0.065Ti wt%. (b) Calculated [7] temperature distribution during spot welding (0.51 mm thick AISI 1008 steel, 4.8 mm diameter electrode with a tip radius of 2.04 mm, 45° electrode taper, welding force of 1.69 kN and a peak current of 8.1 kA. The welding time is a few cycles, where a cycle is the inverse of the current frequency.)

3 Resistance Spot Welding

In resistance spot welding, electrical current flows locally through the two overlapping steel sheets which resist the current and hence become hot. The current is applied via water–cooled copper electrodes which simultaneously apply pressure; this results in the formation of a weld nugget which on cooling provides the required joint. There are typically 3000–5000 of these spot welds in the

Table 1: Typical chemical compositions (wt% / 10^{-3}) of interstitial–free steels.

Type	C	N	Cr	Ni	Si	Mn	Mo	Al	Co	Cu	Nb	Ti	V	S	P	B	Reference
IF–Ti	6	?	3	36	16	183	0	57	6	21	4	65		8	3		[3]
IF–Ti	2	2.8	21	13	11	50		47			1	70		8	7		[4]
IF–Ti	3	3.5	33	12	15	400		36				40		7	6		[4]
IF–Ti	1.4	3.5	20	33	4	205		38		13	2	107	3	10	13		[5]
IF–Ti	5	3.8	15	20	7	195		32		9	1	90	2	9	6		[5]
IF–TiNb	3.3	?	20	21	20	140		7		7	18	18		6.6	13		[5]
IF–TiNbB	3.1	3.4	19	17	11	158		49		10	18	26		5.9	7	0.6	[5]
IF–TiB	2.7	2.4	16	17	5			37		4		75		7	8	10	[5]

manufacture of a single automobile [8–10]. Fig. 2 illustrates a small part of the body of a car during the course of manufacture; the spot welds which are apparent on this would be hidden following manufacture.

Figure 2: An illustration of some of the spot welds providing integrity to the body of a car.

A comparison of the phase diagram with the estimated temperature distribution illustrated in Fig. 1, shows that there is a significant region below the electrode which may momentarily melt, then solidify rapidly under pressure into δ–ferrite; the δ–ferrite on cooling transforms in the solid–state into austenite, which can then develop into a variety of ferritic products on cooling. The heat–affected zone should be rather small according to the temperature field illustrated in Fig. 1b. Note that it is possible, if the cooling rate during solidification is large, for austenite to form directly from the melt instead of the δ–ferrite which would form first during equilibrium solidification [11–14].

Fig. 3a shows a macroscopic image of a spot–welded piece of a titanium–alloyed interstitial–steel. It appears as if the central region which makes up the weld nugget consists of equiaxed grains. This is followed by columnar grains which penetrate into the steel in the heat–affected zone, followed by slightly coarsened grains in the region of the steel which does not become austenitic.

It is suggested that the equiaxed nature of the grains in the nugget are because of the forging action of the weld electrodes where melting presumably also homogenises the temperature field within the fused region. The columnar growth outside of this forged zone follows the direction of heat flow [5, 15, 16]; similar effects are observed when recrystallisation occurs in the presence of a temperature gradient, where the direction of columnar growth can be manipulated by altering that of the temperature gradient [17–19]. Weakness following spot welding is often identified with excessive “grain growth” in the heat affected zone [5, 15, 16].

In its manufactured condition the microstructure of an interstitial–free steel consists of equiaxed

allotriomorphic ferrite grains with a size of the order of 30 µm and a hardness of 80–90 HV. Fig. 3b shows that the hardness recorded in the nugget and the heat–affected columnar zone is greater than that in the unaffected base material. There is therefore a difficulty in interpreting the properties of the weld in terms of excessive grain growth. In fact, what appears to be coarse grains of ferrite contains a much finer microstructure (Fig. 4 [4, 20]) and it would be more reasonable to interpret the macroscopic grains as representing the prior austenite grains. The austenite grains can be large because as demonstrated above (Fig. 1) the TiC particles should be dissolved at temperatures exceeding 950°C.

This interpretation is consistent also with the fact that increasing the manganese concentration from 0.05 to 0.4 wt% leads to a hardness increase in the entire affected zone by about 20–30 HV [4]; manganese has a large effect on hardenability and hence promotes the finer transformation products.

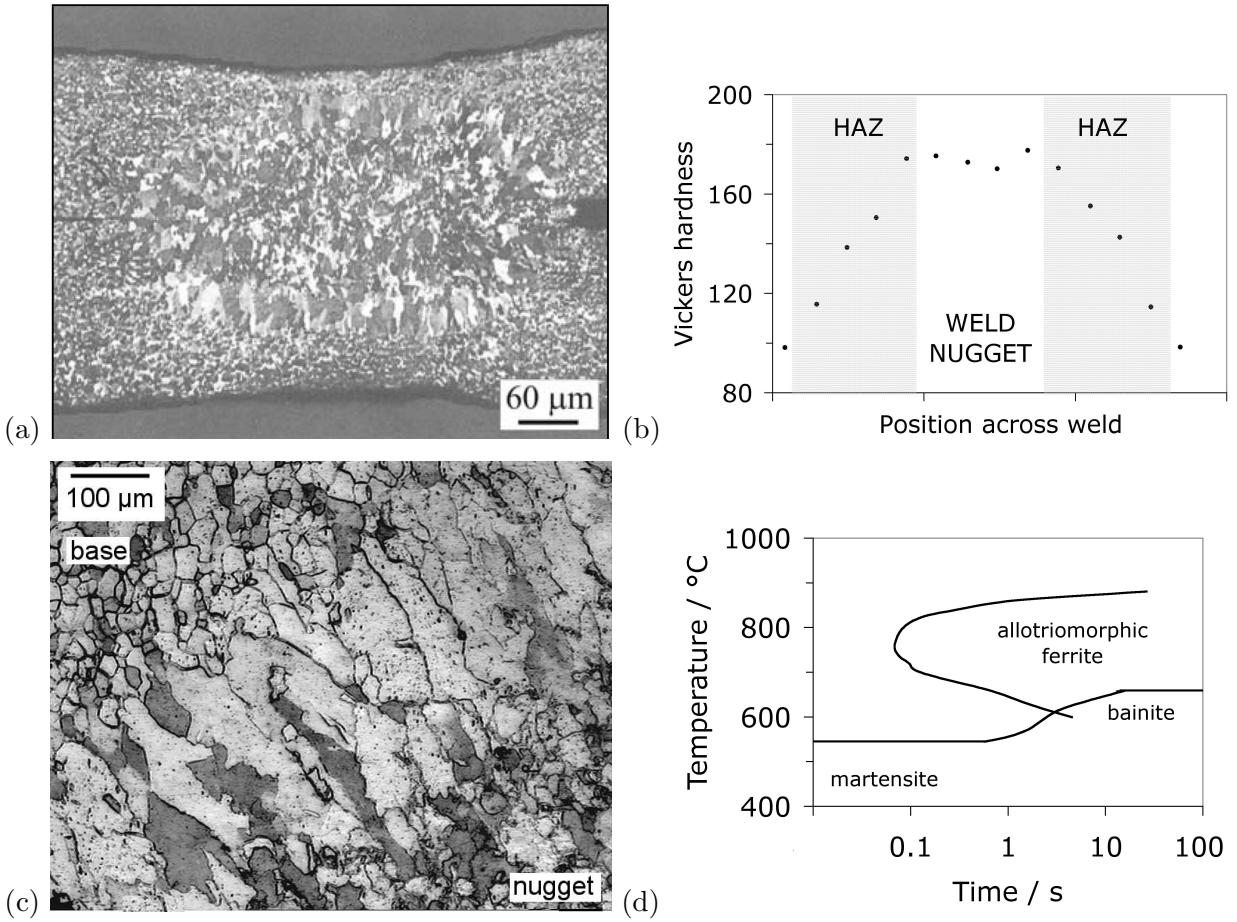

Figure 3: Resistance spot weld produced using interstitial–free steel with 7 kA current, 30 cycles weld time [3] (reproduced with permission of B. Demir). (a) Macrograph showing the weld structure. (b) Corresponding hardness profile across the weld, determined using a Vickers machines with a 200 g load. (c) A higher magnification image of a resistance spot weld on an IF–TiNb steel [5]. Micrograph courtesy of Emin Bayraktar. (d) Calculated time–temperature–transformation diagram for interstitial–free steel with the same composition as that used to calculate the phase diagram in Fig. 1.

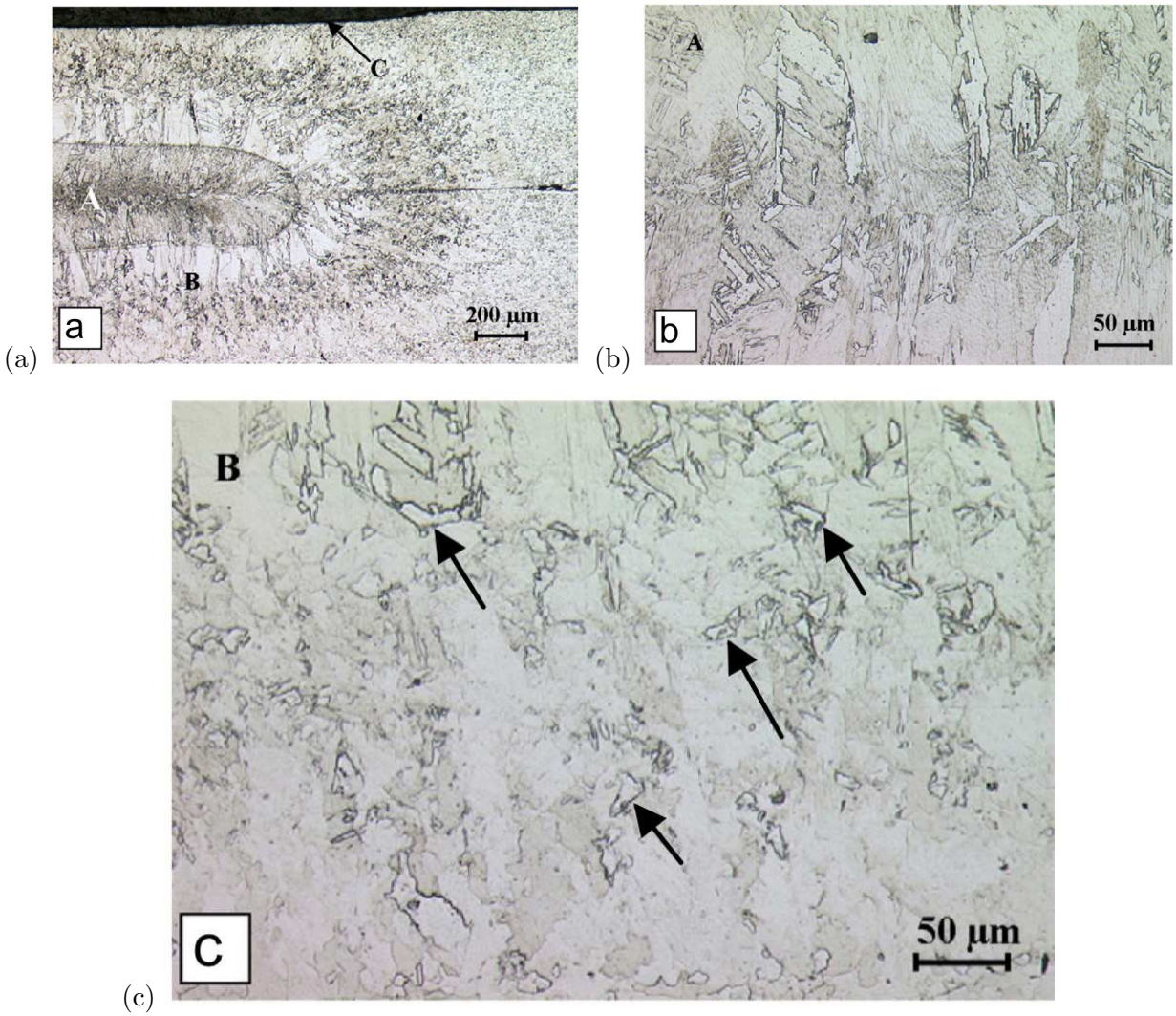

Figure 4: A resistance spot–weld in interstitial–free steel. (a) Low magnification image of weld. 'A' denotes the fusion zone, 'B' the heat–affected zone and 'C' the indentation. (b) The fusion zone. (c) The heat–affected zone; the arrows indicate what appears to be allotriomorphic ferrite. Reprinted from Journal of Materials Processing Technology, Vol. 209, G. Mukhopadhyay, S. Bhattacharya and K. K. Ray, strength assessment of spot–welded sheets of interstitial free steels, pages 1995–2007, Copyright 2009, with permission from Elsevier.

The question then arises as to what the fine microstructure (Fig. 4) within the prior austenite grains of the nugget and columnar HAZ represents. The structures observed have been referred to as 'quasi–polygonal ferrite', bainite and Widmanstätten ferrite [4]. The quasi–polygonal ferrite is defined by reference to a compilation of mixed microstructures obtained using continuous cooling transformation and does not given an indication of a mechanism of transformation.

To elucidate the nature of the fine structures which are harder than the base metal, a time–temperature transformation diagram was calculated for interstitial–free steel as described elsewhere [21–24]. Experimental diagrams of this kind are incredibly difficult to measure for interstitial–free steels because they transform very rapidly. It has been shown for precisely such cases that a calculated diagram can better represent the behaviour of rapidly transforming steels than one which is measured, because it is not possible in the latter case to access isolated reactions due to the high quench–rates required [21].

Fig. 3d shows the calculated time–temperature–transformation (TTT) curves for the initiation of transformation; the martensite–start and bainite–start temperatures are 545 and 659°C respectively and Widmanstätten ferrite is predicted to be absent [25]. The highest temperature at which austenite can transform (into allotriomorphic ferrite) is about 880°C, consistent with Fig. 1. This agreement is expected even though the TTT diagram is calculated assuming paraequilibrium [26–28] because the concentrations of substitutional solutes are in this respect, negligible. The meanings of equilibrium and paraequilibrium become identical when the substitutional solute content becomes zero. It is evident that he formation of allotriomorphic ferrite is extremely rapid and that it is not possible to access the bainite transformation, which is more than an order of magnitude slower. If the cooling rate is fast enough then martensite should be obtained, not bainite.

A fully martensitic sample can only be obtained if allotriomorphic ferrite is avoided with a cooling rate of $1700^\circ\mathrm{C\,s^{-1}}$ according to Fig. 3d. The hardness expected from martensite is, according to [29]:

$$\text{martensite Vickers hardness} = 127 + 949w_{\mathrm{C}} + 27w_{\mathrm{Si}} + 11w_{\mathrm{Mn}} + 8w_{\mathrm{Ni}} + 16w_{\mathrm{Cr}} + 21\log\dot{T} \qquad (1)$$

where the cooling rate $\dot{T}$ is in $^\circ\mathrm{C\,h^{-1}}$ and w represents the weight percent of the solute identified in the subscript. The 95% confidence limits are $\pm 26\,\mathrm{HV}$. Using this equation, the hardness of the fully martensitic state in IF–Ti is found to be $210\pm 26\,\mathrm{HV}$, which is consistent with the peak hardness ($\simeq 180\,\mathrm{HV}$) seen in Fig. 3b. The subsequent decrease in hardness away from the nugget to the base plate could be attributed to the formation of mixtures of martensite and increasing fractions of allotriomorphic ferrite. There is some indication in Fig. 4c that such a mixture does in fact occur in the columnar HAZ.

To summarise, it appears that the microstructure of a resistance spot–welded interstitial–free steel should consist only of two phases, allotriomorphic ferrite and martensite. Bainite is probably too slow to form in these circumstances. The fine structures of the fusion and heat–affected zones illustrated in Figs. 4b,c are consistent with this interpretation since the fusion zone is martensitic whereas the heat–affected zone seems to be a mixture of martensite and allotriomorphic ferrite.

The concepts discussed here would need to be adapted when joining interstitial–free steel to other types of steels, because mixing occurs in the fusion zone that eventually forms the nugget. For example, the resistance spot welding of austenitic stainless steel to IF steel leads to the retention

of austenite in the nugget [30].

4 Conclusions

A method has been outlined to help interpret the development of microstructure when interstitial–free steels are resistance spot–welded. It has been demonstrated, using time–temperature transformation diagram calculations, that certain phases can be ruled out of the microstructure. It seems that the complete description requires only the presence allotriomorphic ferrite and martensite. Bainite is not likely to be present because it forms at a rate which is an order of magnitude slower than allotriomorphic ferrite. Widmanstätten ferrite can similarly be dismissed.

The computer program for the calculation of time–temperature–transformation diagrams can be downloaded freely from

www.msm.cam.ac.uk/map/mapmain.html

Acknowledgment

I am grateful to Dr A. Haldar of Tata Steel for inviting this work, and to Professor Lindsay Greer for the provision of laboratory facilities at the University of Cambridge.

References

[1] T. Araki, K. Shibata, and M. Enomoto. Reviewed concept on microstructural identification and terminology of low carbon ferrous bainites. *Materials Science Forum*, 56–58:275–280, 1989.

[2] T. Araki, M. Enomoto, and K. Shibata. Problems of bainitic transformation and microstructures in low carbon steels. *Testu to Hagane*, 77:1544–1550, 1991.

[3] F. Hayat, B. Demir, M. Acarer, and S. Aslanar. Effect of weld time and weld current on the mechanical properties of resistance spot welded IF (DIN EN 10130–1999) steel. *Kovove Materialy*, 47:11–17, 2009.

[4] G. Mukhopadhyay, S. Bhattacharya, and K. K. Ray. Strength assessment of spot-welded sheets of interstitial free steels. *Journal of Materials Processing Technology*, 209:1995–2007, 2009.

[5] E. Bayraktar, D. Kaplan, L. Devillers, and J. P. Chevalier. Grain growth mechanism during the welding of interstitial free (IF) steels. *Journal of Materials Processing Technology*, 189:114–125, 2007.

[6] NPL. MTDATA. Software, National Physical Laboratory, Teddington, U.K., 2006.

[7] J. Khan, L. Xu, and Y.-J. Chao. Prediction of nugget development during resistance spot welding using coupled thermal–electrical–mechanical model. *Science and Technology of Welding and Joining*, 4:201–207, 1999.

[8] G. Davies. *Materials for Automobile Bodies*. Elsevier Butterworth Heinemann, Oxford, U. K., 2003.

[9] R. W. Rathburn, D. K. Matlock, and J. G. Speer. Fatigue behaviour of spot welded high–strength sheet steels. *Welding Journal, Research Supplement*, 82:207s–218s, 2003.

[10] C. Goldsberry. Resistance welding technology advances. *Welding Magazine*, 80:17–19, 2007.

[11] J. M. Vitek, A. Dasgupta, and S. A. David. Microstructural modification of austenitic stainless steels by rapid solidification. *Metallurgical Transactions A*, 14:1833–1841, 1983.

[12] J. W. Elmer. *Microstructural development during solidification of stainless steel alloys*. PhD thesis, Masschusetts Institute of Technology, Massachusetts, USA, 1988.

[13] H. K. D. H. Bhadeshia, S. A. David, and J. M. Vitek. Solidification sequences in stainless steel dissimilar alloy welds. *Materials Science and Technology*, 7:50–61, 1991.

[14] S. Tsukamoto, H. Harada, and H. K. D. H. Bhadeshia. Metastable phase solidification in electron beam welding of dissimilar stailess steel. *Materials Science & Engineering A*, 178:189–194, 1994.

[15] A. Hasanbasoglu and R. Kacar. Microstructure and property relationships in resistance spot weld between 7114 interstitial free steel and 304 austenitic stainless steel. *Journal of Materials Science and Technology*, 22:375–381, 2006.

[16] A. Hasanbasoglu and R. Kacar. Resistance spot weldability of dissimilar materials. *Materials and Design*, 28:1794–1800, 2007.

[17] M. M. Baloch and H. K. D. H. Bhadeshia. Directional recrystallisation in a nickel base ODS superalloy. *Materials Science and Technology*, 6:1236–1246, 1990.

[18] H. K. D. H. Bhadeshia. Recrystallisation of practical mechanically alloyed iron base and nickel base superalloys. *Materials Science and Engineering A*, A223:64–77, 1997.

[19] C. Capdevila and H. K. D. H. Bhadeshia. Manufacture and microstructural evolution in mechanically alloyed oxide dispersion–strengthened superalloys. *Advanced Engineering Materials*, 3:647–656, 2001.

[20] G. Mukhopadhyay, S. Bhattacharya, and K. K. Ray. Effect of pre-strain on the strength of spot-welds. *Materials & Design*, 30:2345–2354, 2009.

[21] H. K. D. H. Bhadeshia. A thermodynamic analysis of isothermal transformation diagrams. *Metal Science*, 16:159–165, 1982.

[22] J. L. Lee and H. K. D. H. Bhadeshia. A methodology for the prediction of time-temperature-transformation diagrams. *Materials Science and Engineering A*, A171:223–230, 1993.

[23] H. K. D. H. Bhadeshia. The driving force for martensitic transformation in steels. *Metal Science*, 15:175–177, 1981.

[24] H. K. D. H. Bhadeshia. Thermodynamic extrapolation and the martensite-start temperature of substitutionally alloyed steels. *Metal Science*, 15:178–150, 1981.

[25] H. K. D. H. Bhadeshia. Rationalisation of shear transformations in steels. *Acta Metallurgica*, 29:1117–1130, 1981.

[26] A. Hultgren. Isotherm omvandling av austenit. *Jernkontorets Annaler*, 135:403–494, 1951.

[27] M. Hillert. Paraequilibrium. Technical report, Swedish Institute for Metals Research, Stockholm, Sweden, 1953.

[28] H. K. D. H. Bhadeshia. Diffusional formation of ferrite in iron and its alloys. *Progress in Materials Science*, 29:321–386, 1985.

[29] R. Blondeau, Ph. Maynier, J. Dollet, and B. Vieillard-Baron. Estimation of hardness, strength and elastic limit of c- and low-alloy steels from their composition and heat treatment. *Memoires Scientifiques Rev. Metallurg.*, 72:759–769, 1975.

[30] J. B. Lee, D. G. Nam, N. H. Kang, Y. D. Kim, W. Oh, and Y. D. Park. Resistance spot welding of dissimilar materials of austenitic stainless steels and IF (interstitial free) steels. *Korean Journal of Materials Research*, 19:369–375, 2009.